Tubular Reactors for Emulsion Polymerization: II. Model Comparisons with Experiments

D. A. Paquet, Jr. and W. H. Ray
Dept. of Chemical Engineering, University of Wisconsin, Madison, WI 53706

A dynamic model for emulsion polymerization in a tubular reactor has been developed and compared with experimental data. The model uses an axial dispersion coefficient to fit experimentally measured residence time distributions and to represent axial mixing during reaction. Very general emulsion polymerization kinetics are assumed so that a wide range of monomers and operating conditions can be handled. Orthogonal collocation on finite elements was chosen as the numerical solution technique. Comparisons show good agreement between model and experiments for two different monomers.

Introduction

In Part I (Paquet and Ray, 1993), we discuss earlier work using tubular reactors for emulsion polymerization and then present the results of extensive experimental studies. In this article, we develop a model for the tubular reactor and compare model predictions with experimental data. Of the published works discussed in Part I, only *three* modeling studies were reported: the models of Ghosh and Forsyth (1976), the follow-up study by Vatanatham and Forsyth (1979), and the model of Hoedemakers (1990). To the best of our knowledge, these studies represent the complete published efforts to model an open-loop tubular reactor for emulsion polymerization. All of these are steady-state models.

Ghosh and Forsyth (1976) considered a monodisperse particle-size distribution (PSD) in a laminar-flow tubular reactor with radial diffusion. Focusing on nonisothermal operation, they neglected particle nucleation using the number of particles as a parameter in the model. Smith-Ewart case II kinetics (constant radical concentration in the particles) were assumed. The model consisted of an equation for monomer concentration and another for temperature. They compared simulation results with their experiments. In a later article, Vatanatham and Forsyth (1979) explored more parameters and developed guidelines for scaling up a reactor.

Hoedemakers (1990) attempted to model his experimental results in a pulsed packed column. He used axial dispersion to model the mixing in the reactor. Particle nucleation was considered, and Smith-Ewart case II kinetics were used. The resulting model had two state equations, one for particle number and the other for total monomer. A trial-and-error shooting method was used to solve the differential equations.

The model developed in this article will be more general and include the features of the earlier models. In addition, the present model will have more general kinetics and provide dynamic as well as steady-state predictions so that it can simulate a wide range of monomers and operating conditions.

Modeling Equations

A primary issue for modeling a tubular reactor is how to describe the mixing phenomena. Ghosh and Forsyth considered laminar flow with radial dispersion, whereas Hoedemakers used a one-dimensional model with axial dispersion. We have chosen the latter axial dispersion representation for several reasons. First, as shown in Figure 1, an axial dispersion residence time distribution (RTD) model is superior to a laminar-flow RTD for the experimental RTDs presented in Part I. Secondly, dispersion models have been shown to provide an excellent representation of helical tubes and tubes with intermittent mixing points (Stevens and Ray, 1989) for solution polymerization. Thus, we believe an axial dispersion model to be applicable to a wider range of reactors.

The free-radical polymerization kinetics considered in this model are in Table 1. In the reaction scheme, M_n refers to the dead polymer, while P_n represents the live radicals. The modeling equations describing the rates of change of the reactor variables are presented below with a brief description of the physical mechanisms being represented. The mechanisms de-

Correspondence concerning this article should be addressed to W. H. Ray.

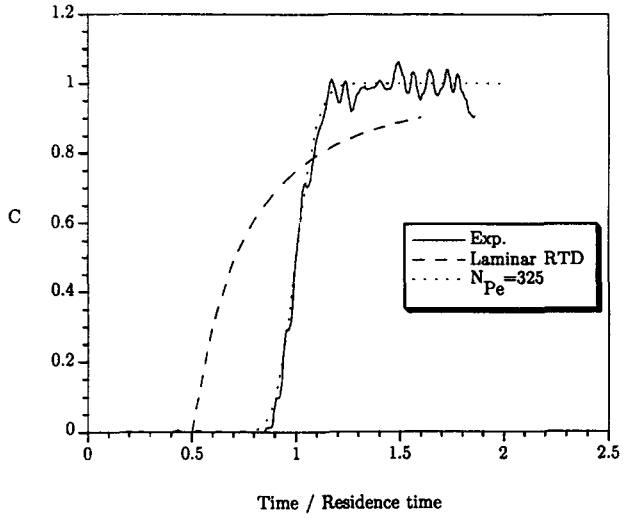

Figure 1. Residence time distribution for a pulsed tubular reactor with mean residence time of 30 min and no pulsation.

Laminar RTD; axial dispersion RTD with $N_{Pe}=325$; experiment.

scribed are similar to those used in the stirred-tank model of Rawlings and Ray (1987a). Constant axial velocity and axial dispersion are assumed as a first approximation to the real behavior. Implementation of the full population balance for the particle-size distribution (PSD) would add a third dimension to the model. To avoid such complexity and in recognition that tubular reactors give rather narrow PSDs, the emulsion particles are assumed monodisperse at any position in the reactor. We write equations for the particle number assuming a micellar nucleation only with a collision model for radical entry ($n=2$):

$$\frac{\partial N_p}{\partial t}+v_z\frac{\partial N_p}{\partial z}-\mathfrak{D}_e\frac{\partial^2 N_p}{\partial z^2}=4\pi r_m^n k_{mm}N_A N_m R_w \tag{1}$$

The polymer produced from the nucleation step is assumed to contribute negligibly to the total polymer mass, so that the mass of polymer, M_p, is given by:

$$\frac{\partial M_p}{\partial t}+v_z\frac{\partial M_p}{\partial z}-\mathfrak{D}_e\frac{\partial^2 M_p}{\partial z^2}=\rho_m g_p k_{po}\phi_m \bar{i} N_p \tag{2}$$

The average swollen particle radius is obtained from the particle number and polymer mass as:

Table 1. Kinetic Scheme for the Model

Initiation:	$I \xrightarrow{k_d} 2R^*$
Propagation:	$P_n^* + M \xrightarrow{k_p} P_{n+1}^*$
Chain transfer:	$P_n^* + M \xrightarrow{k_{trm}} P_1^* + M_n$
	$P_n^* + T \xrightarrow{k_{trt}} T^* + M_n$
Termination:	$P_n^* + P_m^* \xrightarrow{k_t} M_{n+m}$
	or $M_n + M_m$
Inhibition:	$P_n^* + J \xrightarrow{k_j} M_n$

$$r_s=\left(\frac{3}{4\pi\rho_p\phi_p}\frac{M_p}{N_A N_p}\right)^{1/3} \tag{3}$$

A balance on the aqueous-phase free radicals yields:

$$\frac{\partial R_w V_w}{\partial t}+v_z\frac{\partial R_w V_w}{\partial z}-\mathfrak{D}_e\frac{\partial^2 R_w V_w}{\partial z^2}$$
$$=2f_d k_d I V_w-k_j J_w R_w V_w-k_{to}R_w^2 V_w$$
$$-k_{mm}4\pi r_m^n N_A N_m R_w V_w-k_{mp}4\pi R_w N_A N_p r_s^n+D(r_s)N_p\bar{i}. \tag{4}$$

where terms on the righthand side are initiator decomposition, termination with inhibitor, aqueous-phase termination, entry into micelles, entry into particles, and desorption from particles, respectively. The rate of radical desorption is assumed to be (Prindle, 1989):

$$D(r_s)=\frac{\mathfrak{D}_{mm}}{2k_{pm}'}\frac{k_{trm}}{\frac{M_{wtm}\mathfrak{D}_{mm}}{2\rho_m k_{pm}'\phi_m}+r_s^2}+\frac{\mathfrak{D}_{mt}}{2k_{pt}'}\frac{k_{trt}}{\frac{M_{wtm}\mathfrak{D}_{mt}}{2\rho_m k_{pt}'\phi_m}+r_s^2}\frac{C_p}{M_p}. \tag{5}$$

Desorption occurs when a monomeric radical, resulting from a chain transfer event, diffuses from the particle before adding a sufficient number of monomers that render the radical insoluble in the continuous phase.

The average number of radicals per particle is obtained from the familiar Stockmayer-O'Toole solution to the Smith-Ewart recursion relation:

$$\bar{i}=\frac{a}{4}\frac{I_b(a)}{I_{b-1}(a)} \tag{6}$$

where $I_b(a)$ is the modified Bessel function of order b. The order is the ratio of first-order loss (desorption and termination with inhibitor) to termination:

$$b=\frac{2[D(r_s)+k_j J_p]v_s N_A}{g_t k_{to}} \tag{7}$$

The argument is:

$$a=4\left(\frac{k_{mp}4\pi r_s^n R_w v_s N_A^2}{g_t k_{to}}\right)^{1/2}=4\sqrt{\frac{\text{entry}}{\text{termination}}}. \tag{8}$$

It is assumed that initiator is present only in the continuous phase and undergoes first-order decomposition so that its concentration is given by:

$$\frac{\partial I V_w}{\partial t}+v_z\frac{\partial I V_w}{\partial z}-\mathfrak{D}_e\frac{\partial^2 I V_w}{\partial z^2}=-k_d I V_w. \tag{9}$$

There is an additional factor in the Arrhenius expression for the decomposition rate constant:

$$k_d=e_{kd}f_d\exp\left(-\frac{E_{ad}}{R_g T}\right) \tag{10}$$

The factor e_{kd} is used to account for possible enhancements in the decomposition rate due to the presence of surfactant and other species. There has been some controversy over possible enhancement effects. However, the recent experimental results of Okubo et al. (1990) conclude that the effect is negligible. As a result, $e_{kd}=1$ will be used in all simulations.

Surfactant is an inert species in the system so that its concentration is given by:

$$\frac{\partial SV_w}{\partial t}+v_z\frac{\partial SV_w}{\partial z}-\mathcal{D}_e\frac{\partial^2 \mathrm{SV}_w}{\partial z^2}=0. \tag{11}$$

Surfactant adsorption is assumed to be instantaneous, and a surface area balance determines the number of micelles:

$$\frac{4\pi r_m^2 N_m}{a_{em}}=S-S_{cmc}-\frac{4\pi}{a_{ep}V_w}N_p r_s^2 \tag{12}$$

This equation neglects the amount of surfactant adsorbed on the surface of the monomer drops.

Inhibitor can also be present in the reacting emulsion. Consumption by reaction with free radicals occurs in both phases:

$$\frac{\partial J}{\partial t}+v_z\frac{\partial J}{\partial z}-\mathcal{D}_e\frac{\partial^2 J}{\partial z^2}=-k_j J_w R_w V_w-k_j J_p N_p\bar{i}. \tag{13}$$

A simple constant partition coefficient is used to determine the concentration of inhibitor in the aqueous and particulate phases:

$$J_w=m_j J_p. \tag{14}$$

From the total inhibitor balance

$$J=V_w J_w+(1-V_w)J_p \tag{15}$$

one finds

$$J_w=\frac{J}{V_w+(1-V_w)m_j}. \tag{16}$$

A similar treatment is used for chain transfer agent:

$$\frac{\partial C_t}{\partial t}+v_z\frac{\partial C_t}{\partial z}-\mathcal{D}_e\frac{\partial^2 C_t}{\partial z^2}=-k_{trt}g_{tr}C_{tp}N_p\bar{i}. \tag{17}$$

$$C_{tw}=m_t C_{tp}. \tag{18}$$

Just as in the inhibitor equation, the total balance of chain transfer agent is used to obtain the aqueous-phase concentration from the total concentration:

$$C_{tw}=\frac{C_t}{V_w+(1-V_w)m_t}. \tag{19}$$

Mass concentrations and volume additivity are used to determine the mass concentration of water:

$$\sum_{i=1}^{N_{\text{species}}}\frac{m_i}{\rho_i}=1. \tag{20}$$

If the dominant locus of monomer consumption is from reactions within the polymer particles, the partial differential equation for the overall monomer concentration, M, becomes:

$$\frac{\partial M}{\partial t}+v_z\frac{\partial M}{\partial z}-\mathcal{D}_e\frac{\partial^2 M}{\partial z^2}=-\frac{g_p k_{po}\rho_m\phi_m}{M_{wtm}}N_p\bar{i}. \tag{21}$$

The total monomer conversion is defined as the weight fraction of polymer with respect to the total monomer in the feed, or

$$X=\frac{M_p}{M_{wtm}M_f}. \tag{22}$$

When the monomer drops are present, the monomer volume fraction in the particles is at its saturation value.

$$\phi_m=\phi_{m\,\text{sat}} \tag{23}$$

When the monomer drops are not present, the volume fraction is determined by the equilibrium relationship.

$$MV=\frac{\rho_m}{M_{wtm}}\phi_m N_p v_s+M_w V_w V \tag{24}$$

$$M_w=M_{w\,\text{sat}}\phi_m\exp[1-\phi_m+\chi_{mp}(1-\phi_m)^2] \tag{25}$$

Note that the previous equation is based on the equation developed by Morton et al. (1954) for saturated conditions and extended by Min (1978) for conditions less than saturated where the interfacial term, $2\gamma/(R_g T r_s)$ has been neglected. As a result, the monomer volume fraction in the particles is independent of particle size. An energy balance considers thermal axial dispersion and wall heat transfer. Therefore,

$$\overline{mc_p}\frac{\partial(T-T_o)}{\partial t}+v_z\overline{mc_p}\frac{\partial(T-T_o)}{\partial z}-k_e\frac{\partial^2 T}{\partial z^2}=\frac{H_r g_p k_{po}\rho_m\phi_m}{M_{wtm}}N_p\bar{i}-4\frac{U_j}{d_t}(T-T_j) \tag{26}$$

where

$$\overline{mc_p}=\sum_{i=1}^{N_{\text{species}}}m_i c_{pi} \tag{27}$$

and k_e is an effective thermal conductivity.

For all species, a constant initial condition is used.

$$y_i(t<0,\,z)=y_{io}\quad\text{for all } i. \tag{28}$$

Danckwerts boundary conditions are used at the reactor entrance:

$$y_i(t,\,z=0)=y_{if}+\frac{\mathcal{D}_e}{v_z}\frac{\partial y_i}{\partial z}\quad\text{for all } i. \tag{29}$$

Table 2. Conditions for the Continuous Emulsion Polymerizations of Methyl Methacrylate

Variable	Feed	Initial
Monomer Volume Fraction	0.3	0
Temperature (°C)	60	60
Surfactant (mol/L aq)	0.008	0.0
Initiator (mol/L aq)	0.005	0.0

For the energy balance, the effective conductivity replaces the dispersion coefficient. In all simulations, no particles are present in the feed.

A zero gradient is imposed at the reactor exit:

$$\frac{\partial y_i(t, z=L)}{\partial z}=0 \quad \text{for all } i. \tag{30}$$

Solution Techniques

The model contains six to nine partial differential equations (depending on whether inhibitor and chain transfer agent are present and if nonisothermal behavior is permitted) and one nonlinear algebraic equation describing the monomer partitioning. We are interested in the near plug flow limit, since large Peclet numbers (200–600) were obtained in the residence time distribution studies in Part I. Thus, we expect a steep front moving through the reactor during the startup. We have found orthogonal collocation on finite elements capable of resolving the steep front.

To reduce the number of equations, the monomer thermodynamic equilibrium relation was solved internally as needed. Brenan et al. (1989) express strong reservations about solving nonlinear algebraic equations internally and recommend that the algebraic equations be added to equations solved by the integrator. They state that errors from the nonlinear equation solver can cause the integrator to fail. There are several reasons for not following their advice. First, because the equation is distributed, the removal of a state equation can significantly reduce the total number of equations to be solved. Secondly, for a portion of the reactor, the monomer drops are present and the exact solution is known. Lastly,

Table 3. Summary of Parameters for Simulation of Emulsion Polymerization of Methyl Methacrylate

k_{po}	4.92×10^{8} exp $(-4{,}353/R_gT)$ cm³/mol·s (Mahabadi, 1977)
k_{to}	9.8×10^{10} exp $(-701/R_gT)$ cm³/mol·s (Mahabadi, 1977)
k_{trm}	$2.0\times10^{-5}\,k_p$ (Marten, 1980)
k_p'	k_p
k_{mm}	2.0×10^{-5} cm/s (this work)
k_{mp}	2.0×10^{-5} cm/s (this work)
$\mathfrak{D}_{mm}$	1.1×10^{-7} cm²/s (computed from Hansen, 1979; Harada, 1971)
n	2
ρ_m	$0.9659-1.2129\times10^{-3}T+1.6813\times10^{-6}T^2-1.0164\times10^{-8}T^3$ g/cm³ for $0<T<130$°C (Wunderlich, 1975, p. V-77)
ρ_p	$1.195-2.249\times10^{-4}T-1.944\times10^{-6}T^2$ g/cm³ for $0<T<105$°C (Wunderlich, 1975, p. V-76)
$\phi_{m\,sat}$	0.73 (Gardon, 1968)
$[M]_{w\,sat}$	1.49×10^{-4} mol/cm³ (Luskin, 1970)
M_{wm}	100.13 g/mol

Table 4. Gel Effect Parameters for Simulation of Emulsion Polymerization of Methyl Methacrylate

Termination Gel Effect (Ross, 1976)
$g_t = 1.0$ for $v_f \le 0.1731$
$g_t = \exp(75(v_f-0.1731))$ for $v_f \ge 0.1731$
$v_f = 0.025+0.001(T-167)+(0.00048(T-387)-0.001(T-167))(1-\phi_m)$
Propagation Gel Effect (Ballard, 1986)
$g_p = 1.0$ for $w_p \le 0.84$
$g_p = \exp[29.8(w_p-0.84)]$ for $w_p \ge 0.84$
$g_{tr} = g_p$

experience has shown that when the solution from the previous axial point is used as the initial guess to the Newton solver, convergence to a tolerance of 10^{-16} is achieved in fewer than five iterations.

DDASSL (Petzold, 1985) was used as the integrator, and the relative and absolute error tolerances used in the integrator are 10^{-6} and 10^{-8}, respectively. We used the sparse iteration matrix implementation of DDASSL (Marquardt, 1990) to take some advantage of the nearly block diagonal structure of the iteration matrix.

Simulations were performed using orthogonal collocation on finite elements. Cubic polynomials were used with varying number of elements. The experimental conditions of Table 2 were simulated. The parameters used are in Tables 3-5. A residence time of 30 min and a Peclet number of 500 were used to evaluate the solution method.

Figure 2 shows the exit conversion during the startup of the reactor for different numbers of equally-spaced elements. Slight overshoot exists in the 20-element solution. The 40- and 50-element solutions appear to converge. The steady-state particle number profiles are shown in Figure 3. To avoid oscillations, at least 40 elements should be used for this Peclet number.

Simulations were also performed with quadratic polynomials. The startup exit conversion and steady-state particle number are shown in Figures 4-5. It appears that more than 80 elements are needed for a smooth solution; thus, cubic polynomials are to be preferred.

Jensen and Finlayson (1980) derived rules for nonoscillatory solutions of the convection-diffusion equation. For finite elements with two interior points, nonoscillatory behavior is assured when

$$\frac{N_{Pe}\Delta x}{3.64}<1. \tag{31}$$

Table 5. Surfactant and Initiator Parameters for Simulation of Emulsion Polymerization of Methyl Methacrylate

Sodium Dodecyl Sulfate
$[S]_{cmc} = 1.73\times10^{-6}$ mol/cm³ (Schork, 1981)
$r_m = 2.5\times10^{-7}$ cm (Min, 1978)
$a_{em} = 57\times10^{-16}$ cm² (Ahmed, 1971)
$a_{ep} = 57\times10^{-16}$ cm² (Ahmed, 1971)
Persulfate Initiator
$k_d = 1.8\times10^{17}\exp(-34{,}100/R_gT)$ s^{-1} (Kolthoff, 1947)
$e_{kd} = 1.0$
$\eta_d = 1.0$

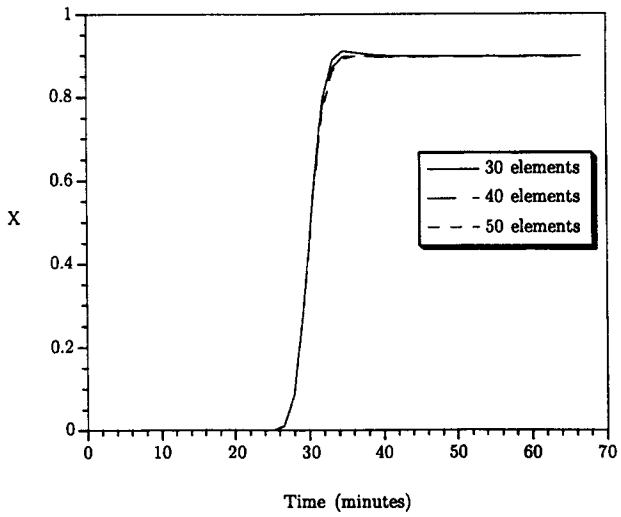

Figure 2. Startup exit conversion vs. time for methyl methacrylate polymerization.

Orthogonal collocation with cubic polynomials on finite elements. $N_{Pe} = 500$. See Table 2 for initial and feed conditions.

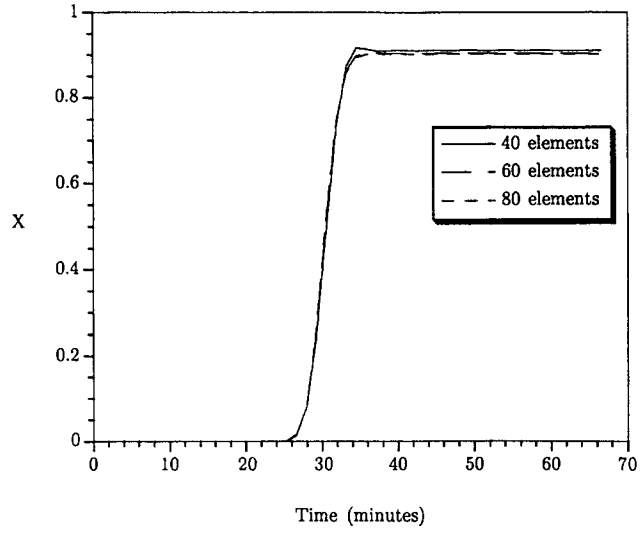

Figure 4. Startup exit conversion vs. time for methyl methacrylate polymerization.

Orthogonal collocation with quadratic polynomials on finite elements. $N_{pe} = 500$. See Table 2 for initial and feed conditions.

For quadratic elements,

$$\frac{N_{Pe}\Delta x}{2} < 1. \tag{32}$$

Using the 40-element solution with the cubic elements and the 80-element solution with the quadratic solution, the values of the lefthand sides of Eqs. 31 and 32 are 4.7 and 4.8, respectively. Finlayson (1992) suggests that while the criteria given guarantee nonoscillatory behavior, acceptable solutions can occur at higher values.

We had explored using moving finite elements (Miller and Miller, 1981) which have been shown to handle moving fronts with few nodes. Unfortunately, the nodes locked onto the startup front and convected down the reactor. This left an insufficient number of nodes to resolve the steep front in the particle number (see Figure 3) that occurs near the entrance of the reactor. Finlayson (1992) has recently reviewed several techniques for solving moving front problems among which OCFEM was listed as a successful method. The adaptive finite element strategies of Wang and Flaherty (1992) represent other methods which appear suited for this problem.

We might have used existing software for solving the set of one-dimensional PDEs. COLNEW (Bader and Ascher, 1987) or EPDCOL (Keast and Muir, 1991) represent two collocation packages that could have been applied. In fact, these packages

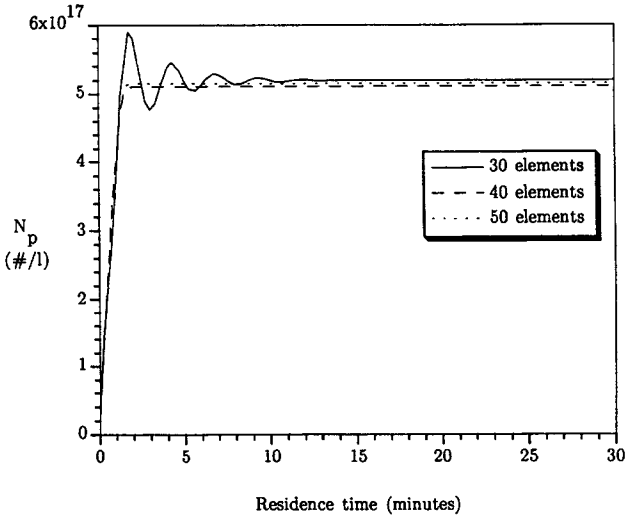

Figure 3. Steady-state particle number vs. average residence time for methyl methacrylate polymerization.

Orthogonal collocation with cubic polynomials on finite elements. $N_{pe} = 500$. See Table 2 for initial and feed conditions.

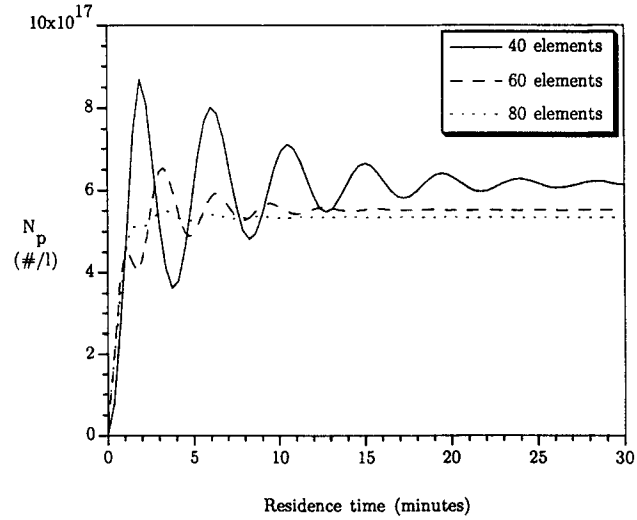

Figure 5. Steady-state particle number vs. average residence time for methyl methacrylate polymerization.

Orthogonal collocation with quadratic polynomials on finite elements. $N_{pe} = 500$. See Table 2 for initial and feed conditions.

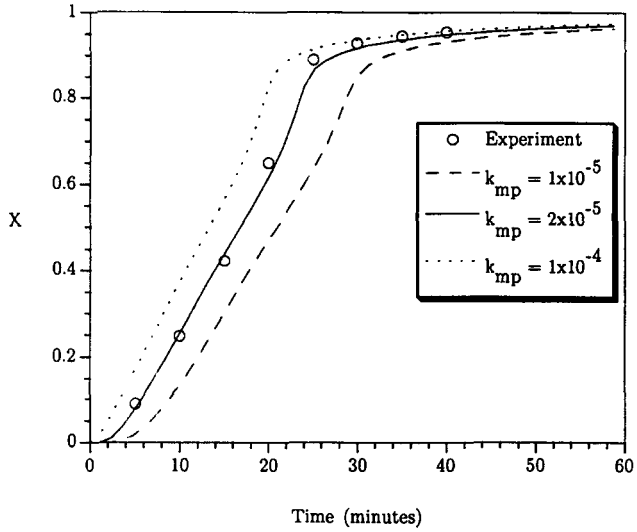

Figure 6. Monomer conversion vs. time for methyl methacrylate polymerization.

o-experimental data. Solid line: $k_{mp}=2\times10^{-5}$. Dashed line: $k_{mp}=1\times10^{-5}$. Dotted line: $k_{mp}=1\times10^{-4}$. The initial conditions were set equal to the feed conditions in Table 2.

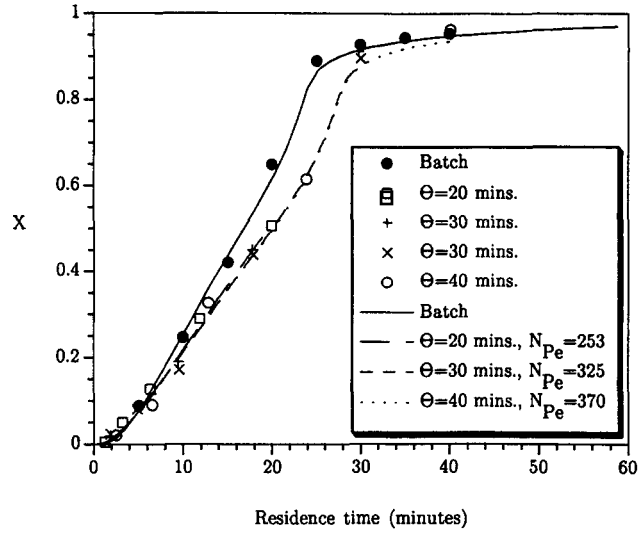

Figure 8. Steady-state conversion vs. average residence time for methyl methacrylate polymerization.

See Table 2 for initial and feed conditions.

invert the block diagonal iteration matrix more efficiently than the sparse matrix implementation of DDASSL. We chose to implement our own solution for the following reasons. Presently, EPDCOL cannot handle nonlinear algebraic equations as state equations. We plan to extend our model to copolymerization in which case it may be beneficial to let the integrator solve the thermodynamic relations. Another interest is implementing the model in our CAD package POLYRED (Ray, 1989). A flowsheet consisting of several tubes in parallel or in series would not generate a block diagonal iteration matrix.

Comparison with Tubular Reactor Experiments

Having determined a numerical method suitable for simulating the tubular reactor, we now compare model predictions with the experimental results in Part 1. We first compared the model of Rawlings and Ray with the batch experimental results. (The initial conditions were equal to the feed conditions in Table 2.) With one exception, all the model parameters were taken from the literature; however, we found it necessary to adjust the entry rate coefficient k_{mp}. Figure 6 shows the conversion histories for different values of the entry rate constant. In all of the simulations, the entry rate coefficient into particles was set equal to the rate coefficient for entry into micelles ($k_{mp}=k_{mm}$). Good agreement with the experimental data is obtained with a value of 2×10^{-5}.

Having established a reasonable set of parameters, simulations were performed with collocation on finite elements with cubic polynomials and 40 equally-spaced elements. The Peclet numbers used were obtained from the residence time distribution studies of Part I. Each dynamic simulation had 726 equations and took approximately 4,000 cpu seconds on a VaxStation 4000 Model 60 to reach steady state.

Figure 7 compares the startup exit conversions for several replicate experiments under the conditions in Table 2. Note that the model with a Peclet number of 325 predicts the "breakthrough" and steady-state conversion very well.

Steady-state conversion predictions from the tubular reactor model with varying experimentally determined Peclet numbers are compared with experimental results at various reactor residence times in Figure 8. For comparison, a corresponding batch reactor experiment and model are also shown. Excellent agreement between the model predictions and experiments is achieved in all cases.

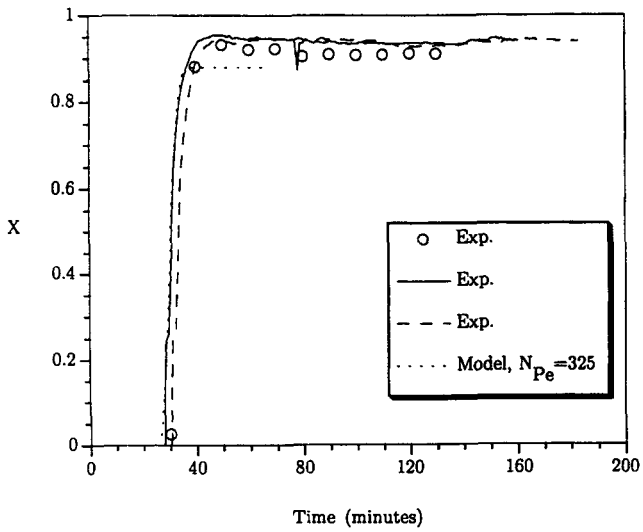

Figure 7. Startup exit conversion vs. time for methyl methacrylate polymerization.

See Table 2 for the initial and feed conditions.

Comparison with Packed Column Experiments of Hoedemakers

The styrene homopolymerization experiments of Hoedemakers (1990) in a pulsed-packed column were used to further test the model. Sodium dodecyl sulfate and sodium persulfate were used as the surfactant and initiator, respectively. Table 6 lists the experimental conditions used by Hoedemakers. Ini-

Table 6. Experimental Conditions for the Styrene Emulsion Polymerizations of Hoedemakers

Variable	Initial
Monomer Volume Fraction	0.3
Temperature (°C)	50
Surfactant (mol/L aq)	0.048
Initiator (mol/L aq)	0.011

tially, simulations were performed with the batch model to match the batch experiment. The parameters used in the simulations are in Tables 7-9. As in the previous case, the entry rate coefficient was the only adjustable parameter.

With these parameters, simulations were performed using the tubular model with varying Peclet numbers. The steady-state conversion profiles are shown in Figure 9. Using Peclet numbers from pulse tracer studies, the model predictions are somewhat lower than the experimental conversions for all Peclet numbers. For example, the simulation with a Peclet number of 50 compares favorably with the experiment with a reported Peclet number of 15. Simulation with a Peclet number of 15 predicts a conversion that is approximately 15% lower than the experimental value at the exit. Obviously, the packed column has less axial mixing during polymerization than reflected in the tracer studies. Hoedemakers does not provide any sensitivity analysis in his Peclet number determination so that the uncertainty in the experimentally determined Peclet numbers is unknown.

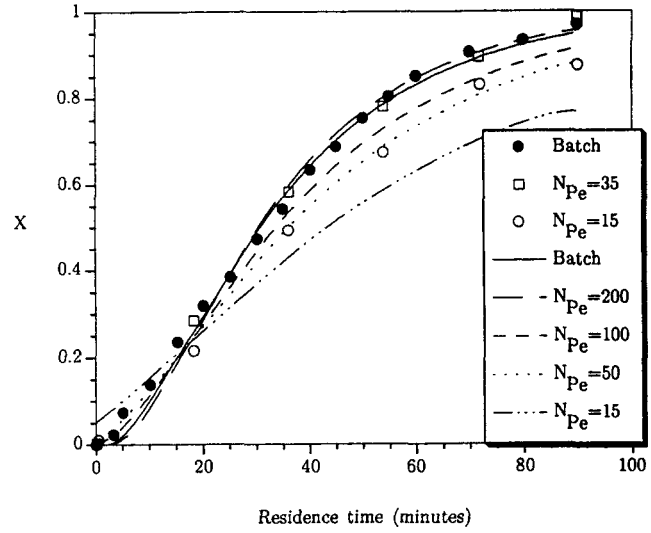

Figure 9. Conversion vs. residence time for styrene polymerization.
See Table 6 for initial/feed conditions.

Table 7. Summary of Parameters for Simulation of Emulsion Polymerization of Styrene

Styrene	
k_{po}	$1.89\times10^{12}\exp(-10{,}400/R_gT)$ cm³/mol·s (Korus, 1975)
k_{to}	$6.52\times10^{16}\exp(-8{,}870/R_gT)$ cm³/mol·s (Korus, 1975)
k_{trm}	$1.0\times10^{-5}\,k_p$ (Harada, 1971)
k_p'	$10\,k_p$ (Lee, 1985)
k_{mm}	2.3×10^{-6} cm/s (this work)
k_{mp}	2.3×10^{-6} cm/s (this work)
$\mathfrak{D}_{mm}$	4.2×10^{-10} cm²/s (Computed from Hansen, 1979; Harada, 1971)
n	2
ρ_m	0.906 g/cm³ (Rudd, 1975)
ρ_p	1.11 g/cm³ (Weast, 1979)
$\phi_{m\,sat}$	0.6 (Gardon, 1968)
$[M]_{w\,sat}$	2.61×10^{-6} mol/cm³ (Min, 1978)
M_{wtm}	104.16 g/mol

Table 8. Gel Effect Parameters for Simulation of Emulsion Polymerization of Styrene

Gel Effect (Friis, 1976; Hui, 1972)	
g_t	$\exp\{-2(b_s x_{loc}+c_s x_{loc}^2+d_s x_{loc}^3)\}$
b_s	$2.57-5.5\times10^{-3}T$
c_s	$9.56-1.76\times10^{-2}T$
d_s	$-3.03+7.85\times10^{-3}T$
g_p	1.0
g_{tr}	g_p

Table 9. Surfactant and Initiator Parameters for Simulation of Emulsion Polymerization of Styrene

Sodium Dodecyl Sulfate	
$[S]_{cmc}$	6.4×10^{-6} mol/cm³ (Gerrens, 1975, pp. II-485-493)
r_m	2.5×10^{-7} cm (Min, 1978)
a_{em}	57×10^{-16} cm² (Ahmed, 1971)
a_{ep}	57×10^{-16} cm² (Ahmed, 1971)
Persulfate Initiator	
k_d	$1.8\times10^{17}\exp(-34{,}100/R_gT)$ s⁻¹ (Kolthoff, 1947)
e_{kd}	1.0
η_d	1.0

Conclusions

A detailed dynamic model for emulsion polymerization in a tubular reactor has been developed and solved using orthogonal collocation on finite elements for a wide range of Peclet numbers. Model predictions were found to compare favorably with emulsion polymerization experiments carried out in tubular reactors, as presented in Part I (Paquet and Ray, 1993). In addition, the model could match the styrene emulsion polymerization data of Hoedemakers (1990) in a pulsed packed column although with some Peclet number modifications. The parameters for both sets of simulations were taken from the literature with only the radical entry rate coefficients fit to the batch experimental results. The model provides a good basis for scaleup design studies and the selection of further pilot-scale experiments in larger diameter tubes.

Acknowledgment

The authors are indebted to the National Science Foundation and the industrial sponsors of the University of Wisconsin Polymerization Reaction Engineering Laboratory for support of this research.

Notation

a = argument for modified Bessel function
a_{em} = area covered by a surfactant molecule on a micelle, cm²
a_{ep} = area covered by a surfactant molecule on a polymer particle, cm²

b = order for modified Bessel function
c_{pi} = heat capacity of species i, cal/g·°C
C = dimensionless salt concentration
C_t = chain transfer agent concentration in the reactor, mol/cm^3
C_{tp} = chain transfer agent concentration in the particles, mol/cm^3
C_{tw} = aqueous-phase chain transfer agent concentration in the reactor, mol/cm^3 water
d_t = tube diameter, cm
D = desorption rate, mol/cm^3·s
$\mathcal{D}_e$ = effective dispersion coefficient, cm^2/s
$\mathcal{D}_{mm}$ = effective diffusivity of monomeric radical in a particle, cm^2/s
$\mathcal{D}_{mt}$ = effective diffusivity of transfer agent radical in a particle, cm^2/s
e_{kd} = initiator decomposition enhancement factor
E_{ad} = initiator decomposition activation energy, cal/mol
f_d = initiator decomposition frequency factor, 1/s
g_p = propagation gel effect factor
g_t = termination gel effect factor
g_{tr} = chain transfer gel effect factor
H_r = enthalpy of polymerization, cal/mol
I = initiator concentration in the reactor, mol/cm^3 water
$I_b(a)$ = modified Bessel function of order b and argument a
$\bar{i}$ = average number of radicals in particles, no./cm^3
J = inhibitor concentration in the reactor, mol/cm^3
J_p = inhibitor concentration in the particles, mol/cm^3
J_w = aqueous-phase inhibitor concentration in the reactor, mol/cm^3 water
k_d = initiator decomposition rate constant, 1/s
k_e = effective thermal conductivity, cal/cm·s·K
k_j = termination with inhibitor rate constant, cm^3/mol·s
k_{mm} = radical entry into micelles rate constant, 1/s
k_{mp} = radical entry into particles rate constant, 1/s
k_p = propagation rate constant, cm^3/mol·s
k_{po} = propagation rate constant at zero polymer concentration, cm^3/mol·s
k'_{pm} = chain transfer to monomer reinitiation rate constant
k'_{pt} = chain transfer to transfer agent reinitiation rate constant
k_t = termination rate constant, cm^3/mol·s
k_{to} = termination rate constant at zero polymer concentration, cm^3/mol·s
k_{trm} = chain transfer to monomer rate constant, cm^3/mol·s
k_{trt} = chain transfer to transfer agent rate constant, cm^3/mol·s
m_i = mass concentration of species i, g/cm^3
m_j = inhibitor equilibrium partition coefficient
m_p = polymer mass in a polymer particle, g
m_t = chain transfer agent equilibrium partition coefficient
M = monomer concentration in the reactor, mol/cm^3
M_p = total polymer mass, g/cm^3
M_w = aqueous-phase monomer concentration in the reactor, mol/cm^3 water
$M_{w\,\mathrm{sat}}$ = aqueous-phase monomer concentration at saturation, mol/cm^3 water
M_{wm} = molecular weight of monomer, g/mol
n = order dependence of radical entry on particle/micelle radius
N_A = Avogadro number
N_m = Micelle number, mol/cm^3 water
N_p = total particle number, mol/cm^3
N_{Pe} = Peclet number
N_{Re} = Reynolds number
r_m = radius of a monomer swollen micelle, cm
r_s = swollen particle radius, cm
R_g = gas constant, cal/mol·K
R_w = aqueous-phase free-radical concentration in the reactor, mol/cm^3 water
S = surfactant concentration in the reactor, mol/cm^3 water
S_{cmc} = critical micelle concentration, mol/cm^3 water
t = time, s
T = reactor temperature, K
T_j = jacket temperature, °C
T_{ref} = reference temperature, °C
U_j = heat-transfer coefficient for transfer to jacket, cal/m^2·s·°C
v_f = free volume
v_m = volume of a micelle, cm^3
v_s = volume of a monomer swollen particle, cm^3
v_z = axial velocity
V_w = water volume fraction, cm^3 water/cm^3
V_{wo} = initial water volume fraction, cm^3 water/cm^3
X = monomer conversion
z = axial coordinate

Greek letters

χ_{mp} = Flory-Huggins interaction coefficient for monomer-polymer
η_d = initiator efficiency factor for producing free radicals, $\eta_d = 1$
γ = interfacial tension between the particle and aqueous phase, dyne/cm
ϕ_m = monomer volume fraction in the particles
$\phi_{m\,\mathrm{sat}}$ = monomer volume fraction in the particles at saturation
ρ_m = monomer density, g/cm^3
ρ_p = polymer density, g/cm^3
θ = mean residence time, s

Literature Cited

Ahmed, S. M., M. S. El-Aasser, F. J. Micale, G. W. Poehlein, and J. W. Vanderhoff, "Rapid Measurement of Adsorption Isotherms of Emulsifiers on Latex Particles," *Polymer Colloids II*, R. M. Fitch, ed., Plenum, New York, 265 (1971).

Bader, G., and U. Ascher, "A New Basis Implementation for a Mixed Order Boundary Value Problem," *SIAM J. Sci. Stat. Comput.*, **8**(4), 483 (1987).

Ballard, M. J., R. G. Gilbert, D. H. Napper, P. J. Pommery, P. W. O'Sullivan, and J. H. O'Donnell, "Propagation Rate Coefficients from Electron Spin Resonance Studies of the Emulsion Polymerization of Methyl Methacrylate," *Macromol.*, **19**, 1303 (1986).

Brenan, K. E., S. L. Cambell, and L. R. Petzold, *Numerical Solution of Initial-Value Problems in Differential-Algebraic Equations*, North-Holland, New York (1989).

Carey, G. F., and B. A. Finlayson, "Orthogonal Collocation on Finite Elements," *Chem. Eng. Sci.*, **30**, 587 (1975).

Finlayson, B. A., *Nonlinear Analysis in Chemical Engineering*, McGraw-Hill, New York (1980).

Finlayson, B. A., *Numerical Methods for Problems with Moving Fronts*, Ravenna Park, Seattle (1992).

Friis, N., and A. Hamielec, "Gel-Effect in Emulsion Polymerization of Vinyl Monomers," *ACS Symp. Ser. Emulsion Polymerization*, **24**, 192 (1976).

Gardon, J. L., "Emulsion Polymerization: VI. Concentration of Monomes in Latex Particles," *J. Polym. Sci.*, **6**, 2859 (1968).

Gerrens, H., and G. Hirsch, *Polymer Handbook*, J. Brandrup and E. H. Immergut, eds., Wiley, New York (1975).

Ghosh, M., and T. H. Forsyth, "Continuous Emulsion Polymerization of Styrene in a Tubular Reactor," *ACS Symp. Ser.*, **24**, 367 (1976).

Hansen, F. K., and J. Ugelstad, "The Effect of Desorption in Micellar Particle Nucleation in Emulsion Polymerization," *Makromol. Chem.*, **180**, 2423 (1979).

Harada, M., M. Nomura, W. Eguchi, and S. Nagata, "Studies of the Effect of Polymer Particles on Emulsion Polymerization," *J. Chem. Eng. Japan*, **4**, 1 (1971).

Hoedemakers, G. F., "Continuous Emulsion Polymerization in a Pulsed Packed Column," PhD Thesis, Univ. of Technology, Eindhoven, The Netherlands (1990).

Hui, A. W., and A. E. Hamielec, *J. Appl. Poly. Sci.*, **16**, 749 (1972).

Jensen, O. K., and B. A. Finlayson, "Oscillation Limits for Weighted Residual Methods," *Int. J. Num. Meth. Eng.*, **15**, 1681 (1980).

Keast, P., and P. H. Muir, "Algorithm 688 EPDCOL: A More Efficient PDECOL Code," *ACM Trans. Math. Soft.*, **17**(2), 153 (1991).

Kolthoff, I. M., and I. K. Miller, *J. Amer. Chem. Soc.*, **69**, 441 (1947).

Korus, R., and K. F. O'Driscoll, *Polymer Handbook*, J. Brandrup and E. H. Immergut, eds., Wiley, New York (1975).

Luskin, L., "Vinyl and Diene Monomers: 1. 3 Acrylic Acid, Methacrylic Acid, and the Related Esters," *High Polymers*, E. Loenard, ed., **XXIV**, 108 (1970).

Lee, H. C., PhD Thesis, Georgia Institute of Technology (1985).

Mahabadi, H. K., and K. F. O'Driscoll, "Absolute Rate Constants

in Free-Radical Polymerization: III. Determination of Propagation and Termination Rate Constants for Styrene and Methyl Methacrylate," *J. Macromol. Sci-Chem.*, **A11**(5), 967 (1977).
Marquardt, W., private communication (1990).
Marten, F. L., and A. E. Hamielec, "High Conversion Diffusion-Controlled Polymerization," *Polymerization Reactors and Processes*, J. N. Henderson and T. C. Bonton, eds., ACS Symp. Ser., Washington, DC, 43 (1979).
Miller, K., and R. Miller, "Moving Finite Elements: I," *SIAM J. Numer. Anal.*, **18**, 1019 (1981).
Min, K. W., and W. H. Ray, "The Computer Simulation of Batch Emulsion Polymerization Reactors Through a Detailed Mathematical Model," *J. of Appl. Poly. Sci.*, **22**, 89 (1978).
Morton, M., S. Kaizerman, and M. W. Altier, "Swelling of Latex Particles," *J. Colloid Sci.*, **9**, 300 (1954).
Okubo, M., and T. Mori, "The Decomposition of Potassium Persulfate Used as Initiator in Emulsion Polymerization," *Makromol. Chem. Macromol. Symp.*, **31**, 143 (1990).
Paquet, D. A., Jr., and W. H. Ray, "Tubular Reactors for Emulsion Polymerization: I. An Experimental Investigation," *AIChE J.*, **40**, 0000 (Jan., 1994).
Petzold, L. R., *DASSL: A Differential-Algebraic System Solver*, Sandia National Laboratories (1985).
Ray, W. H., "Computer-Aided Design, Monitoring, and Control of Polymerization Processes," *Polymer Reaction Engineering*, K. H. Reichert and W. Geisler, eds., VCH Publishers, 105 (1989).
Prindle, J. C., Jr., "Simulation of Emulsion Polymerization in Stirred Tank," PhD Thesis, Univ. of Wisconsin, Madison (1989).
Rawlings, J. B., and W. H. Ray, "The Modelling of Batch and Continuous Emulsion Polymerization Reactors: I. Model Formulation and Sensitivity to Parameters," *Poly. Eng. Sci.*, **28**, 237 (1988).
Ross, R. T., and R. L. Laurence, "Gel Effect and Free Volume in the Bulk Polymerization of Methyl Methacrylate," *AIChE Symp. Ser.*, **72**, 74 (1976).
Rudd, J. F., *Polymer Handbook*, J. Brandrup and E. H. Immergut, eds., Wiley, New York (1975).
Schork, F. J., "The Dynamics of Continuous Emulsion Polymerization Reactors," PhD Thesis, Univ. of Wisconsin, Madison (1981).
Stevens, C. J., and W. H. Ray, "The Mathematical Modeling of Bulk and Solution Polymerization in a Tubular Reactor," *ACS Symp. Ser.*, **404**, 337 (1989).
Vatanatham, T., and T. H. Forsyth, "Scaleup Factors of Tubular Emulsion Polymerization Reactors," *Poly. Eng. Sci.*, **19**(7), 482 (1979).
Wang, Y., and J. Flaherty, "Experiments with an Adaptive H-, P-, and R-Refinement Finite Element Method for Parabolic Systems," *Recent Developments in Numerical Methods and Software for ODEs/DAEs/PDEs*, G. D. Byrne and W. L. Schiesser, eds., World Scientific (1992).
Weast, R. C., ed., *CRC Handbook of Chemistry and Physics*, 60th ed., CRC Press, Boca Raton, FL (1979).
Wunderlich, M., *Polymer Handbook*, J. Brandrup and E. H. Immergut, eds., Wiley, New York (1975).

Manuscript received Apr. 5, 1993, and revision received Oct. 6, 1993.